SSRG International Journal of Electrical and Electronics Engineering
ISSN: 2348-8379/ https://doi.org/10.14445/23488379/IJEEE-V11I1P105

Volume 11 Issue 1, 46-57, January 2024

Original Article

Rapid Video Communication in 5G NR Using Optimised HEVC

K. Maheswari[1], N. Padmaja[2]

[1]*Department of Electronics and Communication Engineering, Jawaharlal Nehru Technological University Anantapur, Andhra Pradesh, India.*
[2]*Department of Electronics and Communication Engineering, Sree Vidyanikethan Engineering College, Affiliated to JNTUA, Andhra Pradesh, India.*

[1]*Corresponding Author: kmaheswari2009@gmail.com*

Received: 16 October 2023 Revised: 18 November 2023 Accepted: 15 December 2023 Published: 20 January 2024

Abstract *- With the steadfast growth of wireless communication technology, multimedia and video have become an integral part of wireless video communication design. A heterogeneous wireless environment is an essential feature of next-generation wireless networks such as 5G. To effectively reduce the complexity updating of the parametric model in the Rate-Distortion (RD) control algorithm in video codec standards, an optimised High-Efficiency Video Coder (HEVC) design is proposed. For a high potential real-time wireless video communication system in 5G, low latency NR-based novel Delay-Distortion-Rate Optimisation (DDRO) control is proposed. The optimised HEVC encoder and decoder are integrated with the DDRO algorithm to make the system highly errorless in the transmission of video frames with low delay. Simulation is performed for the DDRO-HEVC and DDRO-H.264 for comparison of the Key Performance Index (KPI). The result shows that the HEVC with DDRO provides the leading evaluations of the related works of wireless video transmission.*

Keywords *- 5G NR, Wireless video, Y-PSNR, HEVC, Rate optimization, Low latency.*

1. Introduction

There is a widespread need for multimedia streaming in the age of the Internet. Several researchers are working on effective IP network transmission of video quality. Applications for audio and visual communications are provided by multimedia streaming [1]. Delay, jitter, and Peak Signal-to-Noise Ratio (PSNR) are the three most often utilised performance metrics. How do these settings increase the particular Quality of Service (QoS)? In terms of total internet downlink traffic in 2019, video transmission traffic accounted for 60.6% [2]. The explosive development of broadband transfer of video interest and congestion will further encourage AR/VR, 4K/8K, holographic communication, canny metropolises, intellectual carrying, and other technologies [3].

Additionally, the number of video users online has continued to increase quickly, not only as a result of the quick development of traditional network bandwidth but also as a result of the quick development of transportable internet, which includes additional boosted the market prospective for video broadcast.

First, the conventional cinema and television industries have progressively started to promote audio-visual repositories for web videos (including public and private broadcasters). Second, video portals have multiplied (YouTube, Tencent Video, Youku, etc.) [4].

Additionally, the service scope of reputable suppliers of online audio-visual streaming broadcasting also tends to accelerate expansion. As a result, there is now fiercer rivalry among Internet video transmission services. Domestic rivalry is equally intense, with video portals like Youku, iQIYI, and tencent video all putting in their efforts one after the other, despite the fact that these three video portals continue to dominate the domestic video transmission market [5].

Additionally, quickly growing domestically are peer-to-peer video-on-demand services, brief videos, and other services. As a result, the most crucial drive regarding the digital video interaction system may be regarded as determining the ideal video encoder coding configuration that gives the highest video quality while remaining within the allotted toughness economy [6]. The latest version of the video programming technology developed by the ISO/ IEC Moving Picture Experts Group and the ITU-T Video Coding Experts Group (MPEG + VCEG) is called High-Efficiency Video Coding (HEVC) [7]. HEVC is meant to be easily adaptable to all current uses of earlier standards.

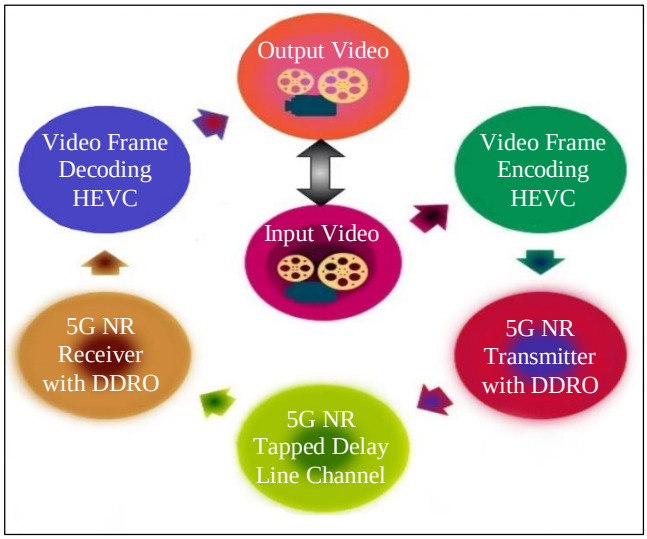

Fig. 1 Proposed block diagram of video transmission over 5G NR using HEVC

The core objective of the recent technology standard is to offer considerably higher firmness ratios than the previous standards, ranging from a 50% bitrate reduction to virtually the same video quality as the H.264/AVC [8]. Even on networks with limited capacity, high-quality video may be sent because of this bitrate decrease. On the other hand, because of its superior high-level syntactic design for identifying the Reference Picture Set (RPS) and creating reference picture lists for inter-picture prediction, HEVC is more resilient to data loss than H.264/AVC [9]. Therefore, HEVC is an excellent contender for wireless applications due to its reduced bitrate and durability against data loss.

The increasing demand for high-quality video streaming has necessitated the development of efficient methods to maintain superior QOS for viewers. Addressing the need to streamline the complexity associated with updating parameter models in RD control algorithms within the video codec standards, a novel approach is presented to optimise the design for streaming video using the HEVC/ H.265 encoder. Specifically tailored for the demands of real-time wireless video communications in 5G.

The proposed optimisation framework enhances the streaming experience by dynamically adjusting encoding parameters based on network conditions and viewer preferences. In this work, we discuss Low Delay and Low Distortion (LDLD) optimisation using an HEVC encoder for the 5G New Radio (NR) wireless Video communication (ViNR) system. In this model, the TDL channel is configured with a Delay-Distortion-Rate Optimization (DDRO) algorithm.

To create an entirely different video deformation model, the HEVC encoder model is combined with the transmission deformation model, as shown in Figure 1. The 5G NR wireless video communication system's functionality is then optimised, and resources are distributed using the established framework. An expedited approach to the optimisation challenge is put forth based on how the HEVC encoder behaves in order to arrive at the ideal coding configuration.

The remaining sections of the paper adhere to this structure as follows: Section 2 delves into related works, while Section 3 pronounces the HEVC encoder model and the 5G NR DDRO algorithm. Section 4 extends the evaluation of the proposed system through analysis and discussion of the performance results. The conclusion was detailed in section 5.

2. Related Works

A number of techniques, such as a quick set of rules for the most critical modulus for video encoders [11], as well as low-difficulty encoder design [10], were created to lower the cost of video encoding due to demographics. The early CU quad-tree termination technique, which restricts the HEVC coding framework's flexibility while saving a substantial amount of computation, is the most often used technique to simplify the HEVC encoder [12].

These algorithms are unable to change their responses to the resources that are available, which vary among systems. Even when resources for distortion corrections are available, this causes video aberration in such algorithms. On the other hand, none of these methods will be able to cut computation any more than what they now do.

In [13], an analytical framework is created by including power consumption in the conventional rate-distortion theory. For a primary MPEG-4 encoder, the power rate and distortion structure are erected in two parts. The first step is to create a power-mountable video encoding structural design employing a variety of control settings. To create the power rate and distortion model, it is second to analyse each control parameter of the R-D behaviour.

When it comes to power-mountable video encoding, the P-R-D architecture offers a solid recommendation. Other video coding standards like H.264 and HEVC cannot be used with this technology; however, By providing an operational P-R-D analysis to produce an analytical P-R-D model for portable video communication devices [14] and performance analysis of wireless video sensor networks, the same authors expanded on their previous work.

A comparison of rate-distortion and complexity between HEVC and AVC codecs is given in [15]. The most challenging modules are the inter-prediction ones. According to the results. [8] Evaluate the HEVC encoder's encoding efficiency and computational complexity. Each encoding parameter's impact on complexity, bitrate, and PSNR variations is assessed, and each coding tool's impact on encoder behaviour is recorded with the addition of many additional coding tools

linked to the HEVC flexible coding structure, a comparable study is offered in [16]. Using the findings of this investigation, an intricate regulator for the HEVC encoder is developed for real-time applications.

In a recent research paper [24], an in-depth examination of error performance was presented, encompassing key metrics such as PSNR, BER and Throughput. These metrics play a crucial role in assessing the resilience needed for support, all of which are critical for determining the robustness of supporting applications involving low-delay video delivery. Moreover, researchers dedicated their efforts to developing an efficient error resilience algorithm for H.265/HEVC. This algorithm [25] focuses on automatically identifying and safeguarding the most active frame regions from transmission errors. However, it comes with a trade-off, as it leads to an increase in both the encoding bit rate overhead and the computational complexity of encoding /decoding.

The analysis of the literature highlights the importance of adopting efficient and effective strategies to tackle critical challenges in wireless video communications, including efficient video compression, low latency and high data rates. The combination of 5G NR and HEVC creates a synergetic impact on these challenges. This integration not only enhances user experience but also establishes a foundation for pioneering applications and services in future.

3. Proposed Work

This part details the proposed Low Delay Low Distortion (LDLD) optimisation using HEVC in the 5G ViNR algorithm. Combining motion-compensated prediction with transform coding for high-efficiency coding is how the HEVC handles coding. The block-based hybrid coding structure is the term used to describe this kind of coding. Figure 1 shows a schematic of a HEVC encoder. The HEVC encoder differs from earlier standards in that it uses a configurable quad-tree coding block partitioning structure. Additionally, motion estimation, intra-prediction and Context-Adaptive Binary Arithmetic Coding (CABAC) have been enhanced along with parallel processing.

I, P and B - frames are the three types of hybrid video coding frames that might be used, depending on the coding circumstances [17]. An intra-coded frame is one with I. No more frames are needed for the encoding to take place. The I-frame establishes random access points along the stream and serves as a reference frame for forecast frames. Complete reference frames have this characteristic; hence, they often require the most bits. An anticipated frame is a p-frame. To fully decode it, a reference frame is required. A P-frame can also include picture data and motion correction. A projected frame is the B-frame. Reference frames for this frame may be from the past or the future.

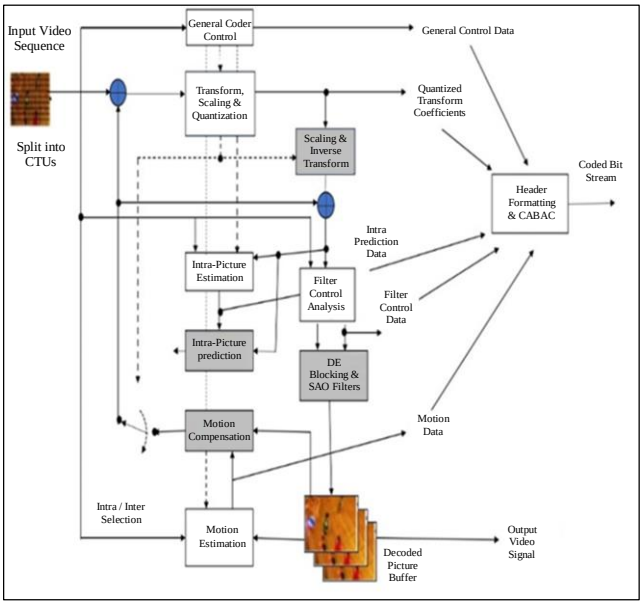

Fig. 2 HEVC encoding and decoding

Additionally, it might serve as a frame of reference. Out of the three frame kinds, it uses the fewest bits. Group of Pictures (GOP) is the term used to describe the three different frame types that make up a compressed video stream.

The input video is initially divided into equal-sized pieces known as Coding Tree Blocks (CTB), as shown in Figure 2, for the HEVC procedure. Compression and decoding are processes that happen in every CTB. The smaller blocks, referred to as Coding Units (CU), are sub-partitioned into which a CTB is divided. The fundamental building elements of prediction are the CUs.

Inter-prediction and intra-prediction represent two conceivable forms of prediction. By employing compressed and decoded data from the block consideration, intra-prediction is executed for the corresponding video frame. Inter-prediction benefits the frames next to it. It uses motion compensation and can make predictions based on areas that are comparable across previously coded frames. Motion compensation is the name given to this method. Prediction is done to eliminate repetition in the current frame as well as in subsequent frames [18].

Following prediction, residuals are derived by subtracting the predicted and original data. These leftovers must then be compacted. The Discrete-Fourier Transform (DFT) is applied to them. The residuals are transformed into the frequency domain via DFT. A transformation matrix is quantised in order to lose unnecessary information. After quantisation, the leftover information and procedures are used for entropy coding, resulting in a compressed bit stream. Therefore, integer DFT and quantisation are the only processes that result in data loss.

The exact opposite procedure is carried out on the decoder side. To recover residuals, de-quantisation and inverse DFT are used. The restored pixel values are then calculated by adding the residuals and anticipated values. These recovered data from the current frame are used for intra-prediction. An extra step can be used to eliminate the blackness that the DFT and quantisation processes caused. The Decoded Picture Buffer (DPB) stores the repaired and enhanced video frame for inter-prediction between succeeding frames.

3.1. HEVC Prediction

Given that both employ spatial sample-based predictions, HEVC intra-prediction may be seen as an expansion of H.264/AVC intra-prediction. The following are the fundamental components of constructing intra-prediction in HEVC:

1. A coding scheme called quad-tree.
2. Production of comparable samples for DC prediction.
3. Creating smooth sample surfaces using planar prediction.
4. 33 different prediction directions for angular prediction.
5. Smoothing reference samples.
6. Boundary sample filtering.

Due to attempts to forecast samples in various directions and careful consideration of how to create a smoother zone with progressively varying sample values, HEVC intra-prediction has increased efficiency in comparison to earlier standards [19].

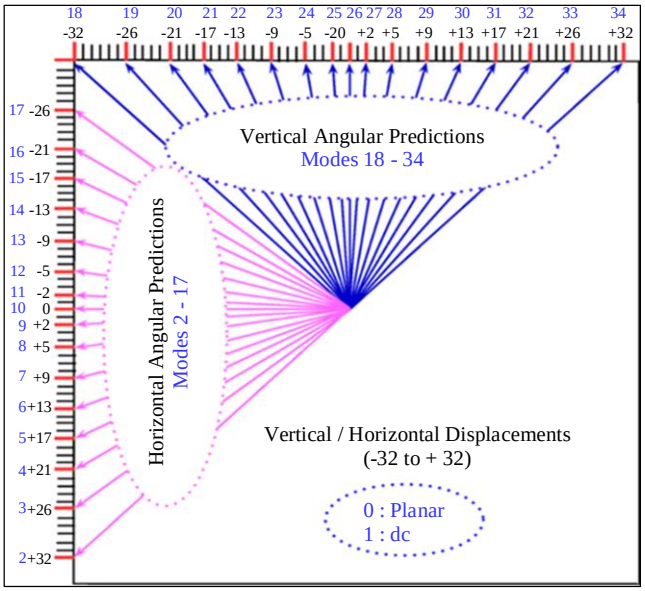

Fig. 3 Prediction modes of HEVC

Predictions are made by calculating the correlation between blocks that are geographically adjacent. Figure 3 illustrates the 33 various directional orientations. Planar and DC prediction modes are furthermore provided in addition to these. The amplitude surface with horizontal and vertical scope is assumed in planar prediction. DC prediction, on the other hand, presupposes a level surface with a value that corresponds to the mean value of boundary samples.

2 to 17 angular modes use left reference samples, whereas 18 to 34 angular modes use top reference samples and projected sample locations in a single line. In this method, negative indices of projected reference pixels occur in a few instances where a negative intra-prediction angle is present.

3.2. Optimisation of Rate Control in HEVC

The two phases of a rate control method are typically various unit's rate allocation process and using the R-D model to determine the encoding parameter. The typical method for creating a rate allocation methodology is to solve the related R-D optimisation problem. The model of rate distortion, which describes the allocation of the rate, places a high priority on the rate distortion link. The responses to the rate distortion optimisation issue can be found based on the provided rate distortion model. On the basis of convex optimisation theory, the proposed optimisation challenge will be condensed. A two-stage bisection method-based methodology is also developed to discover the solution. The hyperbolic R-D model utilised in H.265/ HEVC [20] is first briefly reviewed.

$$D = C \cdot R^{-K} \tag{1}$$

Wherein the computational factors for the video material's properties are C (C > 0) and K (K > 0). Mean Square Error (MSE) and permitted bit rate per pixel (bpp) are used to determine D and R, respectively. Conferring to the RDO principle, the slope of the rate Distortion curve is λ. Over and done with Equation (1), λ can be articulated as,

$$\lambda = \frac{\partial D}{\partial R} = -C * K * R^{-K-1} \tag{2}$$

By means of adjusting the value of λ from the above equation, we can able to perform rate control. The granted rate is then established the coding parameter λ is,

$$\lambda_i = \mathbb{E}(C_i * K_i * R_i^{-K-1})$$

$$= \sum_{l=1}^{L_i} \sum_{j=1}^{J_i} C_{i,j} * K_{i,l} * R_i^{-K_{i,l}-1} * A'_{i,j} * B'_{i,j} \tag{3}$$

Additionally, QP may be calculated using the QP-connection in [21]. The rate distortion model's preliminary facts are equivalent to those in [22]. The halting bisection method's empirical parameters can be determined depending on the distortion degree and the desired bit rate of a few preliminary tests on a typical test video sequence. The assigned CTU bit rate can be found by resolving the relevant decision-making issue prior to encoding CTUs in the current frame. Then, based on the remaining rate budget, the assigned

bit rate for each CTU is modified. Following CTU encoding, the R-D model parameters may be updated using the distortion and actual bit rate of each CTU.

3.3. Delay-Distortion-Rate Optimization Based Resource Allocation and Scheduling in Sub Slices

Due to the substantial unpredictability of user portrait and channel characteristics in sub-slice, in 5G NR, resource optimisation was performed with respect to the separation methodology. As a result, isolation must be maintained so that when there are differences in the profiles, allocating system resources to one sub-slice does not affect the performance of the other sub-slices. Let us say totally 'M' sub-slices, represented by M_1,...M_s, and 'V' users per sub-slice, represented by U_1,..., U_s. If S and U are the number of sub-slices (M) and users set (V) respectively.

To find the Pareto optimum solution, we employed shared models so that the decision-maker could interrelate with the approach [23]. After determining the best S-RS needed to estimate, DDRO allocates S-RS resources to users per sub-slice in order to guarantee SLAs for average latency, distortion, and service rate. We outline the goal of reducing the average latency across sub-slices per network slice in this section,

$$max \sum_{m=1}^{S} \sum_{i=1}^{U(m)} a_{i,m}(t) \quad (4)$$

Where, $a_{i,m}(t)$ represents the throughput of the service based on the perception of each user related to at least one service. $rn_{i,m}$ denotes the quantity of resources in the evident of the fluctuating radio resources, S_{max} is maximum number of sub slices per network slice, In each sub-slice, the average delay for each user is $D_{i,m}$,and the maximum tolerable delay T_D is in the middle of user equipment and generation node. To maximise the service throughput of users in all sub slices, it will be calculated using the above equation. To perform the maximisation process, need to figure out the optimum service throughput mentioned as $a_{i,m}(t)$ to be constructed each user of each sub slices.

$$a_{i,m}(t) = \frac{\left((v_{i.m}T_0 - LO_{i,m}) * S_{i,m} * 8\right)}{T_0 * \left[2 - (1 - B_i m)^{S_{i,m} * 8}\right]} \quad (5)$$

Where, in m^{th} sub slice, the i^{th} user's fluctuating packet transmission rate (1/sec) is $v_{i,m}$, $s_{i,m}$ is packet size represented in bytes, T_o is transmission delay and each sub slice the user distortion is denoted as $LO_{i,m}$, $B_{i,m}$ is beamforming vector ,to calculate the average delay (D_m) with respect to optimum service throughput, the $r_{i,m}$ calculation methodology as follows,

$$r_{i,m} = \frac{\left(\rho_{i,m} * \left\{a_{i,m}(t) * \left[2 - (1 - B_{i,m})^{S_{i,m} * 8}\right] + \frac{LO_{i,m} * S_{i,m} * 8}{T_0}\right\}\right)}{L_{i,m}} \quad (6)$$

Where, $L_{i,m}$ is the packet length, and $\rho_{i,m}$ is link utilisation. The average delay derived is,

$$D_m = \frac{\left(\lim_{t \to \infty} \frac{1}{t} \sum_{\tau=0}^{t-1} \left[\sum_{i=1}^{U(m)} E\{Q_{i,m}(\tau)\}\right]\right)}{\sum_{i=1}^{U(m)} r_{i,m}} \quad (7)$$

Where, $Q_{i,m}(\tau)$ is the m^{th} sub slice i^{th} user current data queue at that time of, τ encoding the Equation (5), we get hold of optimum user service throughput per sub-slice across the fluctuating sub slices.

4. Results and Discussion

4.1. Experimental Setup

The simulation performance for video transmission in the 5G NR platform using optimised HEVC is described in this section. To validate the algorithm, the hardware configurations use Inter (R) Core (TM) i5-3470 with a main frequency of 3.2 GHz memory of 4GB; the software configurations include MATLAB 2020a version, which is used as an experimental platform.

We compared our proposed model of DDRO (HEVC) and DDRO (H.264) with specific state-of-art methods of dRDO, JM, delay-Power-Rate-Distortion (dPRD), rate control algorithm for delay-penetrating video streaming (DA), cross-layer optimised (CA) distortion, bit rate, Y-PSNR and time consumption are the critical parameters of the evaluation in this simulation. Videos of bus, container, foreman and mobile with AVI format are used for testing in the experiment.

These videos include the object motion effects of high motion, complex motion, slow motion and stable motion. Also, it has the camera effects of dynamic position of the camera and zooming impact. Bus video has a resolution of 352x288 with 36.5 Mbps data rate and 15fps. Container, foreman and mobile videos are captured with the exact resolution of 256x128. The data rates of these three videos are 1.8 Mbps, 1.7 Mbps and 3.3 Mbps respectively. 30 fps is the same frame rate of container, foreman and mobile videos.

The simulation setups in environment variables and the configured values are as follows: the search block size of each frame is 16, and the typical frame resizing dimension is 128x128x3. The third dimension of each frame size represents the RGB colour framed processing in our work to show the compatibility to the real-time scenarios. A transport block size of 2856 Bytes is set in the configuration. For the 5G NR model, the subcarrier space of 15 KHz with 52 resource blocks and 16 HARQ is fixed. LDPC transmission coding scheme is selected, and in decoding LDPC, the Layered Belief Propagation (LBP) method is chosen. For channel PUSCH, the TDL channel is constituted with a delay spread of 30ns, maximum doppler spread of 10Hz, code rate 193/1024 and slot-wise DM-RS mapping.

4.2. Performance of Optimisation in Encoding

The two different encoders of optimisation are compared in this work named, H.265 (HEVC) and H.264. Figure 4 shows the end-to-end distortion as the metric of Mean Square Error (MSE) with different Packet Error Probability (PEP). The conventional performance metric of wireless video communication is end-to-end distortion. Also, the Mean Square Error is calculated in the middle of the original frame to the corresponding reconstructed frame at the decoder [2], [5]. The end on distortion D_E^K for the K^{th} frame is denoted as follows,

$$D_E^K = D_S^K + D_T^K \quad (8)$$

Where the source coding distortion D_S^K of the K^{th} frame was affected due to the quantisation error at that time of lossy video compression and transmission distortion D_T^K of the K^{th} The frame fluctuated with respect to transmission error due to bandwidth deviation and packet losses. Low distortion denotes the highly efficient coding scheme in the system.

In Figure 4, two different λ = {2, 4}, QP = {24, 40} values are considered for the illustration of the impact of encoding parameters on the distortion of H.264 and H.265 coders. As the search size of λ and Quantization Parameter (QP) decreases, the End to End distortion gets reduced in both cases of H.264 and H.265. With our proposed H.265 coder optimisation, 3 and 25 MSE is attained at 0% and 20% of PEP with {λ, QP} = {2, 24}which is 38% less distortion than H. 264 coder.

Figure 5 elucidates the efficiency of the ideal objective value's convergence D (λ_τ, 〖QP〗 _τ), a sub-problem with a variety of initial point choices (λ_0, QP〗 _0), which indicates the computational compatibility of proposed HEVC based DDRO in 5G NR video transmission for foreman video sequence. For {λ_0, QP〗 _0} = {12,22} and {λ_0, 〖QP〗 _0} = {8,10}, the optimisation converged at the 5-th iteration itself with starting MSE of 5.8 and 7.9 respectively. However, with {λ_0, QP〗 _0} = {2,1} of lowest values, the starting MSE is 0, and it is converged at the 6th iteration.

4.3. Performance of Average Y-PSNR with Different Initial Channel State Index

The Peak Signal-to-Noise Ratio (PSNR) measured between the luminance component of an image before the encoding and the image after the decoding is termed Y-PSNR. Different initial channel states are configured, and optimal values are shown to correspond to the maximum Y-PSNR with the foreman video sequence. Figure 6 depicts the performance of Y-PSNR for different ranges of channel code rate r of HEVC and H.264 coder in a 5G NR optimised video transmission system model. It is transparently shown that in Figure 6, for each starting channel state with regard to the peak average Y-PSNR, the optimal channel coding rate r* can be attained. The transmission distortion will be condensed by way of less source coding distortion when r > r*. When the coding rate is limited to r < r*, it increases the distortion and reduces the Y-PSNR simultaneously.

Initial channel state indices considered in this work are 1,3,5. When the initial channel state index is reduced to 1, the Y-PSNR will be reduced. Along with these three state index performances, the steady-state curve is also shown in Figure 5, which illustrates that the channel impulse behaviour lies on the centre point of the three curves.

Figure 7 illustrates the liaison in the middle of the end-to-end delay-bound ΔT_max-d_c and the average end-to-end Y-PSNR with channel capacity Rc = 100Kbps and frame interval Tf = 0.3s. These graphical results prove that as the delay bound increases, the Y-PSNR will increase because less packet loss occurs when buffering packets take place.

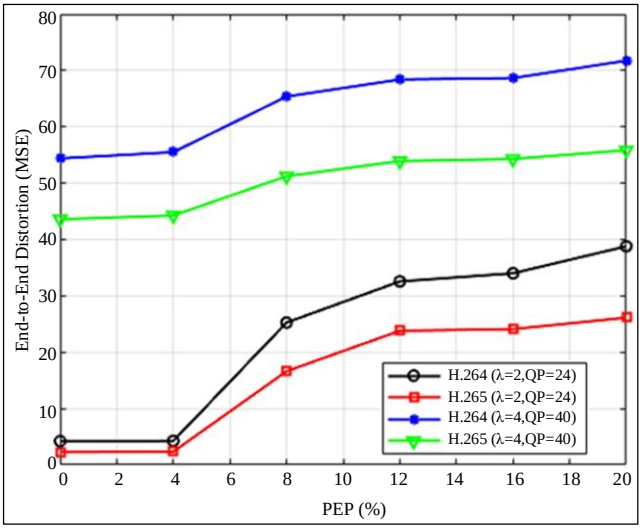

Fig. 4 End-to-end distortion versus PEP

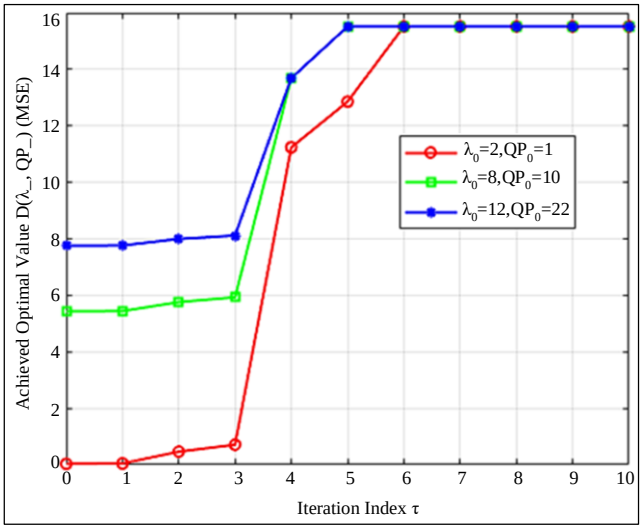

Fig. 5 Convergence behaviour of optimisation

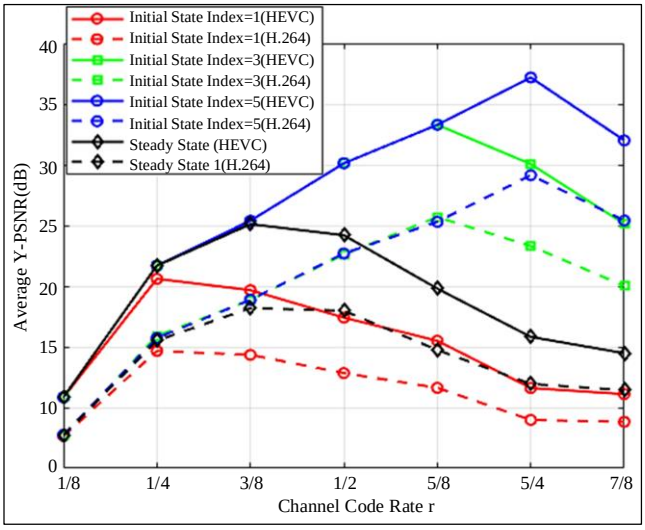

Fig. 6 Influence of various channel code rates

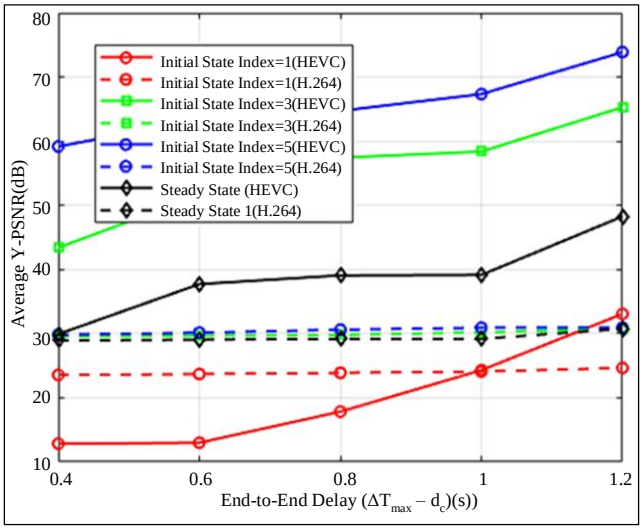

Fig. 7 Different end-to-end delay bounds' effects $\Delta \mathbf{T_{max}} - \mathbf{d_c}$

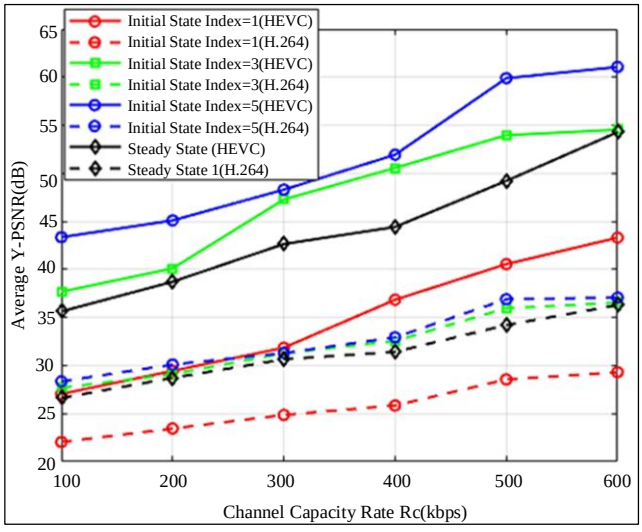

Fig. 8 Impact of different channel capacities R_c

In H.264 coding, the Y-PSNR increment scale is very low. In HEVC, for every delay-bound increment factor, the scaling of increment in Y-PSNR increases, as shown in Figure 6. This figure shows three different initial channel state indexes of 1, 3, and 5, as well as a steady state.

For these four cases, the Y-PSNR of HEVC is 74dB, 66dB, 33dB and 50dB, respectively, at a delay bound of 1.2s. For H.264, 30dB, 28dB, 24dB and 28.5dB, the ICS index is 1, 3, 5 and steady state correspondingly. As channel capacity increases, the Y-PSNR will be increased by means of each frame supported by a large amount of source coding and channel, which results in low-distorted received video frames.

This affiliation is shown in Figure 8 for HEVC and H.264 with multiple initial channel state indices. Out of four cases in the graph, when initial state index=5, HEVC achieves the Y-PSNR of 61dB at Rc = 600Kbps; at the same point, H.264 attains the 37dB of Y-PSNR which is 40% lower Y-PSNR than the HEVC coder.

4.4. Comparison of Baseline Schemes with Proposed Model

With receiver SNR of 2dB, the encoding bit rate of each frame ranges from 1-125 for different baseline schemes and proposed DDRO with H.264 and HEVC for foreman sequence are shown in Figure 9.

To determine the optimal channel code rate of the LDPC block code through the DDRO and also the merging of H.264 and H.265 (HEVC) coder to obtain the most effective compromise among the available source coding rate vs. redundancy rate imposed by channel coding, here JM and dPRD schemes fail.

In particular, the DDRO is able to determine an ideal channel code level for each GOP in consideration of the time-varying channel situation. As DDRO adaptively selects the optimal code rate for each GOP, the encoding bit rate will be higher than that of existing methods. In DDRO with H.264 and HEVC coder, the encoding bit rate is achieved at 7.98 Gbps and 1.25 Gbps, respectively. This bit rate is 50% higher than the JM and DA methods. CA algorithm attains the lowest bit rate of 0.3 Gbps.

The encoding time for each method is shown in Figure 10. The optimisation of the coder of DDRO will increase the encoding time compared to other non-optimisation methods like JM and DA. However, when we have an HEVC coder, the delay for the encoding will be too low compared to H.264.

Thus, it has a low encoding time of not more than 80ms, which is five times less than DDRO with an H.264 encoder. The overall calculation time for each technique takes into account both the time spent on optimisation during the successive process for choosing the most suitable parameters and the time involved in encoding the order of events.

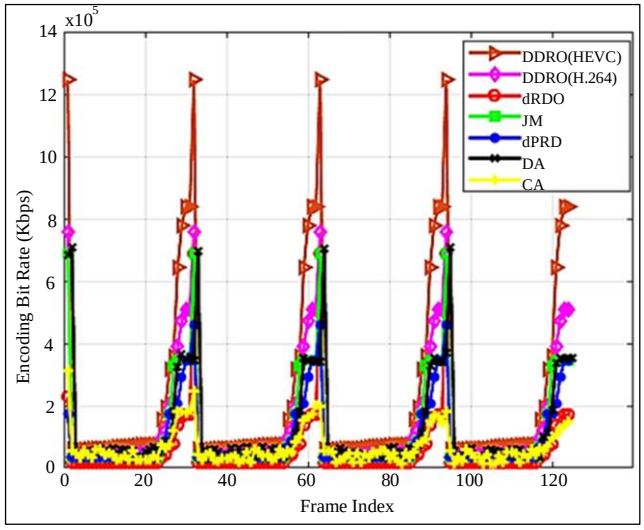

Fig. 9 Encoding bit rate vs. Frame index

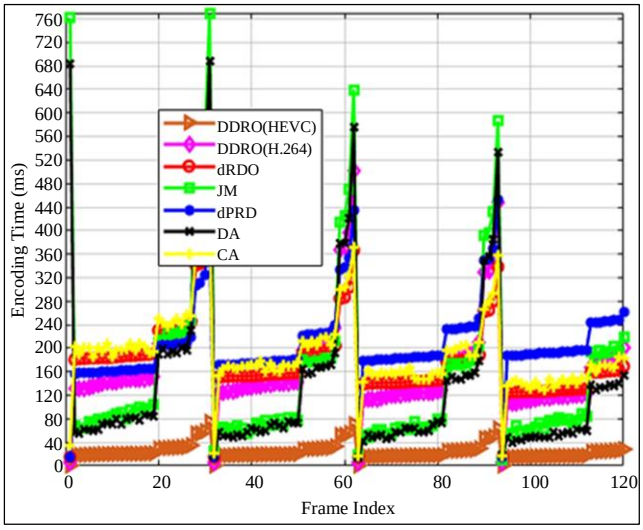

Fig. 10 Encoding time vs. Frame index

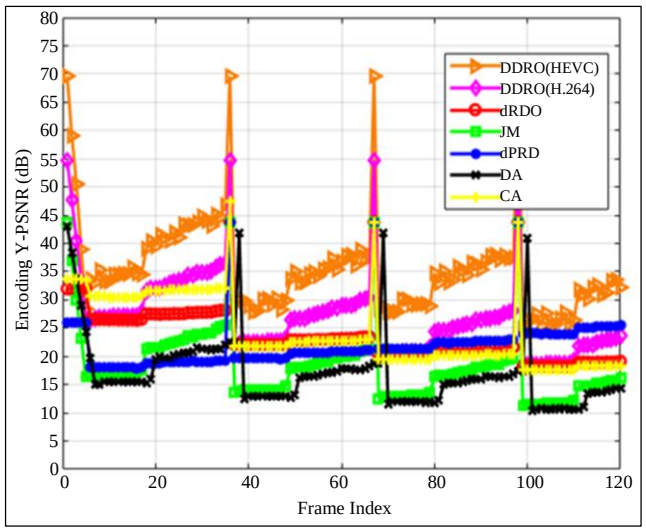

Fig. 11 Encoding Y-PSNR vs. Frame index

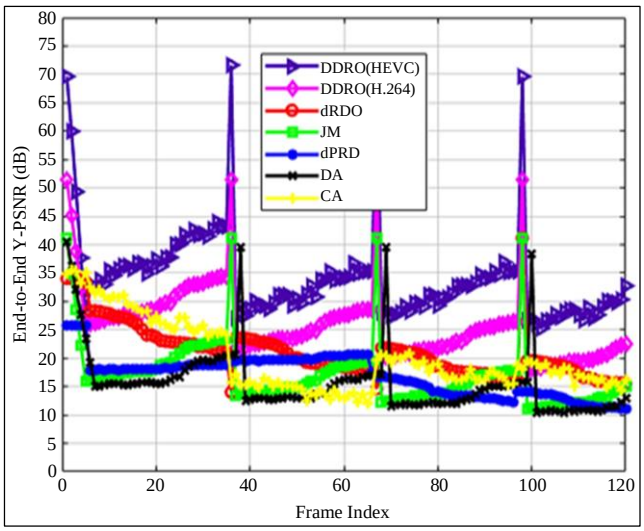

Fig. 12 End-to-end Y-PSNR vs. Frame index

Accordingly, Table 1 indicates that the calculation time per frame is calculated by averaging the combined amount of the optimisation time and the complete encoding time throughout all frames. These two distinct kinds of time are required for each practical algorithm operation. From Figure 11, within a particular GOP, it can be observed that a greater encoding bit rate typically leads to a more excellent encoding Y-PSNR, indicating that a higher channel code rate is given to that GOP to enhance the available source coding rate.

The peak encoding Y-PSNR for DDRO (H.264) is 55dB, and DDRO (HEVC) is 70dB, which is 22% higher than the H.264 coder and 35% higher than JM. As the encoding Y-PSNR increases, the source coding-based distortion will become very low, and the optimisation will reduce the transmission distortion in the 5G NR protocol. Thus, it will reflect in the end-to-end Y-PSNR to a high value of 72dB for DDRO (HEVC) and 51dB for DDRO (H.264), as depicted in Figure 12. For Different SNRs and different Rc, mean Y-PSNR is calculated and shown in Table 2 with the comparison of baseline methods.

5. Conclusion

In this work, the HEVC-based optimised DDRO control algorithm is integrated into 5G NR video communication. The HEVC prediction model and optimisation of the Rate-Distortion (RD) model are presented.

The DDRO-NR algorithm with HEVC and H.264 coders is designed and evaluated with multiple scenarios in the simulation section. Most probably, Y-PSNR, End-to-End distortion, encoding bit rate and time complexity are the critical point metrics for performance analysis.

The best Y-PSNR and low distortion is attained with DDRO (HEVC) and DDRO (H.264) compared to the other

earlier implemented methods. Compared to H.264, the HEVC coder provides a low delay of 0.05s as well as a high Y-PSNR of 70dB with a less distortion rate of 28 (MSE).

Acknowledgements

The authors thank the faculty of ECE, JNTUA, and Ananthapuramu for their constant support.

References

[1] M. Sheik Dawood et al., "Performance Analysis of Efficient Video Transmission Using EvalSVC, EvalVid-NT, EvalVid," *Material Today Proceedings*, vol. 46, no. 9, pp. 3848-3850, 2021. [CrossRef] [Google Scholar] [Publisher Link]

[2] Nan Hu et al., "A Novel Video Transmission Optimization Mechanism Based on Reinforcement Learning and Edge Computing," *Mobile Information Systems*, vol. 2021, pp. 1-10, 2021. [CrossRef] [Google Scholar] [Publisher Link]

[3] Arvin Ghotbou, and Mohammad Khansari, "VE-CoAP: A Constrained Application Layer Protocol for IoT Video Transmission," *Journal of Network and Computer Applications*, vol. 173, 2021. [CrossRef] [Google Scholar] [Publisher Link]

[4] Jia Luo et al., "Adaptive Video Streaming with Edge Caching and Video Transcoding over Software-Defined Mobile Networks: A Deep Reinforcement Learning Approach," *IEEE Transactions on Wireless Communications*, vol. 19, no. 3, pp. 1577-1592, 2020. [CrossRef] [Google Scholar] [Publisher Link]

[5] Liu Chun, and Dong Yuning, "QoE-Aware Video Transmission Optimization Method for Joint Rate Control and Buffer Management in LTE Networks," *Journal of Nanjing University of Posts and Telecommunications*, vol. 3, pp. 59-67, 2016. [CrossRef] [Publisher Link]

[6] Ji Yan Wu, Kaishun Wu, and Ming Wang, "Power-Constrained Quality Optimization for Mobile Video Chatting with Coding-Transmission Adaptation," *IEEE Transactions on Mobile Computing*, vol. 20, no. 9, pp. 2862-2876, 2021. [CrossRef] [Google Scholar] [Publisher Link]

[7] Milad Abdollahzadeh et al., "Optimal HEVC Configuration for Wireless Video Communication under Energy Constraints," *IEEE Access*, vol. 6, pp. 72479-72493, 2018. [CrossRef] [Google Scholar] [Publisher Link]

[8] Zhi Ma, and Songlin Sun, "Research on HEVC Screen Content Coding and Video Transmission Technology Based on Machine Learning," *Ad Hoc Networks*, vol. 107, 2020. [CrossRef] [Google Scholar] [Publisher Link]

[9] Mateus Grellert et al., "Complexity Control of HEVC Encoders Targeting Real-Time Constraints," *Journal of Real-Time Image Processing*, vol. 13, pp. 5-24, 2017. [CrossRef] [Google Scholar] [Publisher Link]

[10] Anil Kumar Budati et al., "Optimized Visual Internet of Things for Video Streaming Enhancement in 5G Sensor Network Devices," *Sensors*, vol. 23, no. 11, pp. 1-17, 2023. [CrossRef] [Google Scholar] [Publisher Link]

[11] Milad Abdollahzadeh, Hamed Alizadeh Ghazijahani, and Hadi Seyedarabi, "Quality Aware HEVC Video Transmission over Wireless Visual Sensor Networks," *2016 24th Iranian Conference on Electrical Engineering (ICEE)*, Shiraz, Iran, pp. 787-792, 2016. [CrossRef] [Google Scholar] [Publisher Link]

[12] Hamed Alizadeh Ghazijahani et al., "Adaptive CSK Modulation Guaranteeing HEVC Video Quality over Visible Light Communication Network," *2016 8th International Symposium on Telecommunications (IST)*, Tehran, Iran, pp. 789-794, 2016. [CrossRef] [Google Scholar] [Publisher Link]

[13] Junaid Tariq, Sam Kwong, and Hui Yuan, "Spatial/Temporal Motion Consistency Based MERGE Mode Early Decision for HEVC," *Journal of Visual Communication and Image Representation*, vol. 44, pp. 198-213, 2017. [CrossRef] [Google Scholar] [Publisher Link]

[14] Tao Zhang et al., "Fast Intra-Mode and CU Size Decision for HEVC," *IEEE Transactions on Circuits and Systems for Video Technology*, vol. 27, no. 8, pp. 1714-1726, 2017. [CrossRef] [Google Scholar] [Publisher Link]

[15] Renjie Song, and Yuandong Zhang, "Optimized Rate Control Algorithm of High-Efficiency Video Coding Based on Region of Interest," *Journal of Electrical and Computer Engineering*, vol. 2020, pp. 1-17, 2020. [CrossRef] [Google Scholar] [Publisher Link]

[16] Yanchao Gong et al., "Temporal Layer-Motivated Lambda Domain Picture Level Rate Control for Random-Access Configuration in H.265/HEVC," *IEEE Transactions on Circuits and Systems for Video Technology*, vol. 29, no. 1, pp. 156-170, 2019. [CrossRef] [Google Scholar] [Publisher Link]

[17] Junaid Mir, Dumidu S. Talagala, and Anil Fernando, "Optimization of HEVC λ-Domain Rate Control Algorithm for HDR Video," *2018 IEEE International Conference on Consumer Electronics (ICCE)*, Las Vegas, USA, pp. 1-4, 2018. [CrossRef] [Google Scholar] [Publisher Link]

[18] Vijayalakshmi S. Patil, and Suvarna Nandyal, "Video Compression Using H.265 (HEVC-Main Profile)," *International Journal of Applied Engineering Research*, vol. 17, no. 4, pp. 427-435, 2022. [Google Scholar] [Publisher Link]

[19] Shanshe Wang et al., "Rate-GOP Based Rate Control for High Efficiency Video Coding," *IEEE Journal of Selected Topics in Signal Processing*, vol. 7, no. 6, pp. 1101-1111, 2013. [CrossRef] [Google Scholar] [Publisher Link]

[20] Bin Li et al., "QP Refinement According to Lagrange Multiplier for High Efficiency Video Coding," *2013 IEEE International Symposium on Circuits and Systems (ISCAS)*, Beijing, China, pp. 477-480, 2013. [CrossRef] [Google Scholar] [Publisher Link]

[21] Miaohui Wang, King Ngi Ngan, and Hongliang Li, "Low-Delay Rate Control for Consistent Quality Using Distortion-Based Lagrange Multiplier," *IEEE Transactions on Image Processing*, vol. 25, no. 7, pp. 2943-2955, 2016. [CrossRef] [Google Scholar] [Publisher Link]

[22] Hao Zeng, and Jun Xu, "Rate Control Technology for Next Generation Video Coding Overview and Future Perspective," *Electronics*, vol. 11, no. 23, pp. 1-22, 2022. [CrossRef] [Google Scholar] [Publisher Link]

[23] Sharvari Ravindran et al., "Required Delay-Based Network Sub-Slices Resource Optimization for 5G Radio Access Network," *2019 IEEE International Conference on Advanced Networks and Telecommunications Systems (ANTS)*, Goa, India, pp. 1-6, 2019. [CrossRef] [Google Scholar] [Publisher Link]

[24] Maheswari K., and Padmaja Nimmagadda, "Error Resilient Wireless Video Transmission via Parallel Processing Using Puncturing Rule Enabled Coding and Decoding," *e-Prime - Advances in Electrical Engineering, Electronics and Energy*, vol. 6, pp. 1-12, 2023. [CrossRef] [Google Scholar] [Publisher Link]

[25] Taha T. Alfaqheri, and Abdul Hamid Sadka, "Low Delay Error Resilience Algorithm for H.265|HEVC Video Transmission," *Journal of Real-Time Image Processing*, vol. 17, pp. 2047-2063, 2020. [CrossRef] [Google Scholar] [Publisher Link]

Appendix

Table 1. Comparison of actual computation time

Video Sequences	Algorithms	Optimisation Time (s)	Encoding Time (s)	Computation Time per Frame (s)
Bus	DDRO-HEVC	0.584	4.61	0.025
	DDRO-H.264	2.74	21.96	0.131
	dRDO	5.80	22.56	0.21
	JM	0	21.08	0.16
	dPRD	1.23	22.48	0.18
	DA	0.06	21.15	0.16
	CA	7.05	22.26	0.22
Foreman	DDRO-HEVC	0.59	8.87	0.059
	DDRO-H.264	3.08	45.16	0.251
	dRDO	7.27	46.89	0.33
	JM	0	45.96	0.28
	dPRD	1.72	46.20	0.29
	DA	0.23	45.96	0.28
	CA	8.76	46.35	0.33
Mobile	DDRO-HEVC	0.74	4.82	0.041
	DDRO-H.264	3.73	23.62	0.228
	dRDO	6.67	22.89	2.10
	JM	1.16	21.93	0.58
	dPRD	2.94	23.14	1.01
	DA	0.87	22.20	1.33
	CA	8.48	23.38	0.95

Container	DDRO-HEVC	0.66	6.42	0.067
	DDRO-H.264	3.40	31.02	0.37
	dRDO	6.51	32.27	1.08
	JM	0.38	31.21	0.53
	dPRD	2.20	31.46	0.49
	DA	0.35	30.65	0.24
	CA	7.36	31.87	0.59

Table 2. Comparison of baseline methods

Video Sequence	Avg. SNR (dB)	Rc (Kbps)	DDRO-HEVC	DDRO-H.264	dRDO	JM	dPRD	DA	CA
Bus	2	100	31.22	28.91	24.13	19.72	20.07	22.97	23.60
		200	33.96	29.04	27.36	21.11	21.97	26.79	26.65
		500	38.91	35.88	33.40	24.15	24.77	32.77	32.59
	5	100	33.79	29.93	26.36	22.41	22.65	24.03	25.50
		200	38.05	33.39	30.47	24.20	24.62	27.52	29.38
		500	43.73	38.75	37.49	27.71	28.13	36.5.	36.37
	10	100	35.09	30.01	28.47	19.00	18.09	26.71	27.64
		200	39.64	34.66	32.71	19.41	18.69	31.59	31.97
		500	55.78	46.82	42.52	19.89	19.77	42.15	41.60
Foreman	2	100	39.44	33.18	30.87	25.65	25.71	29.47	30.07
		200	41.39	35.93	33.79	26.95	26.94	32.82	33.14
		500	48.20	39.99	37.59	28.33	28.11	37.02	36.91
	5	100	43.18	35.74	33.15	28.96	28.74	32.05	32.22
		200	46.72	38.33	36.38	30.29	30.08	35.82	35.40
		500	51.33	42.44	40.51	31.79	31.57	40.30	39.50
	10	100	45.17	38.00	35.10	24.37	24.28	34.21	33.57
		200	47.80	39.97	38.21	24.75	24.62	37.84	37.69
		500	53.68	45.02	42.50	25.20	25.00	41.96	41.85
Mobile	2	100	30.76	23.39	20.34	18.27	17.98	19.58	19.85
		200	35.75	26.14	22.96	18.98	18.85	22.51	22.41

		500	38.59	27.88	25.98	20.58	20.25	24.87	25.77
	5	100	32.09	23.46	21.84	20.25	19.93	21.51	21.34
		200	37.92	26.69	24.18	21.52	21.20	23.67	23.44
		500	40.41	30.03	28.85	23.99	23.82	28.15	28.26
	10	100	32.53	25.57	23.29	17.79	17.37	22.99	22.63
		200	39.41	29.37	25.75	18.18	17.89	25.30	25.38
		500	48.85	34.41	32.56	19.02	18.89	31.64	31.26
Container	2	100	37.26	25.91	22.72	22.58	22.91	22.84	19.01
		200	39.27	28.36	24.56	21.35	25.86	25.89	21.36
		500	45.91	29.30	28.79	24.15	30.69	29.19	24.86
	5	100	35.03	26.47	23.62	22.03	24.40	25.72	20.90
		200	39.52	29.95	27.43	26.11	28.27	29.91	22.61
		500	41.11	35.38	33.36	30.28	33.59	36.52	26.75
	10	100	34.39	29.99	26.13	21.59	26.82	27.90	22.11
		200	40.45	32.07	30.28	28.00	30.95	32.16	24.90
		500	49.08	41.60	39.92	33.57	40.65	41.12	30.28